WORLD JOURNAL OF PHARMACY AND PHARMACEUTICAL SCIENCES
SJIF Impact Factor 7.421
Volume 7, Issue 11, 131-142 Research Article ISSN 2278 – 4357

3D QSAR STUDIES OF BENZIMIDAZOLE DERIVATIVES AS FtsZ INHIBITORS

Kavan M. Jani*

Institute of Pharmacy, Nirma University, Ahmedabad, Gujarat, India.

Article Received on
31 August 2018,

Revised on 21 Sept. 2018,
Accepted on 12 Oct. 2018,

DOI: 10.20959/wjpps201811-12586

***Corresponding Author**
Kavan M. Jani
Institute of Pharmacy, Nirma University, Ahmedabad, Gujarat, India.

ABSTRACT

Tuberculosis is one of the most infectious disease in the world. Filamentous Temperature Sensitive Mutant Z gene (FtsZ) being a strong target implies an efficacious therapy for tuberculosis treatment. Amongst the entire moieties which are currently under research, Benzimidazole plays a vital role in the field of drug discovery and development. In the current paper, Three dimensional quantitative structure activity relationship (3D QSAR) studies were performed on 2,5,6- tri-substituted benzimidazole derivatives. The studies were carried out to know the structural requirements of Filamentous Temperature Sensitive Mutant Z gene (FtsZ) agonists. Using various techniques the model possessed high arithmetical reliability and good predictive power. Consequently, the results obtained may provide important information in further optimization of benzimidazole derivatives as Filamentous Temperature Sensitive Mutant Z gene (FtsZ) agonists.

KEYWORDS: Filamentous Temperature Sensitive Mutant Z gene (FtsZ), Comparative Molecular Field Analysis (CoMFA), Comparative Molecular Similarity Indices Analysis (CoMSIA).

INTRODUCTION

Tuberculosis, caused by Mycobacterium Tuberculosis (M.TB) is a leading cause of mortality around the world.[1] Despite of the fact, insights appears that around 32% of the world's population is contaminated by this disease. Now-a-days, it is noted that more individuals are contaminated from tuberculosis than ever before.[2] Due to expanded microbial resistance new classes of anti-mycobacterial targets with novel components are today's ought to battle against the multi-drug diseases.[3] An unused targets are needed that will be helpful to shorten the length of chemotherapy. Therefore, a keen interest has concentrated on five membered

heterocyclic compounds like imidazole, pyrrole, oxadiazole, traizoles and other heterocyclic derivatives have been detailed. Indeed it can be known that the azole derivatives provides a new class that are effective drugs, which is reported to restrain microscopic organisms by blocking the bio-synthesis of certain bacterial liquids and mechanism of action.[4]

In this context, Filamentous Temperature Sensitive Mutant Z gene (FtsZ) being a pre-requisite bacterial cytokinesis protein, is a highly promising therapeutic target. Figure.1, it can be known that in presence of GTP, Filamentous Temperature Sensitive Mutant Z gene (FtsZ) polymerises bi-directionally at the centre of the cell wall on the internal layer to form a dynamic helical structure known as the Z-ring, this results into septum arrangement and cell division. Bacterial growth and cell cessation takes place when the blockage of septum formation occurs. Eventually, cell division also results, during an inhibition assembly.[5]

Scaffolds of benzimidazole are considered as one of the favoured structure in the field of medicinal chemistry. Undoubtedly, it can be known from the survey that different scaffolds are developed, which sums-up into exhibiting biological activities.[3,6] Although several researches are going on, thereby some reports are available on anti-TB activity.[1] Based on CoMFA, accompanying CoMSIA methods are helpful in determining 3D-QSAR methods for the SAR of 2,5,6-tri-substituted benzimidazole compounds are to be examined. In addition to it information can be fetched, based on 3D-QSAR studies, which results into further structure based drug design process. From the study it can be known that it will bestowed the execution for the further design of selective and potent Filamentous Temperature Sensitive Mutant Z gene (FtsZ) agonists.[7] The workflow of Filamentous Temperature Sensitive Mutant Z gene (FtsZ) mechanism is in the Fig. 1.

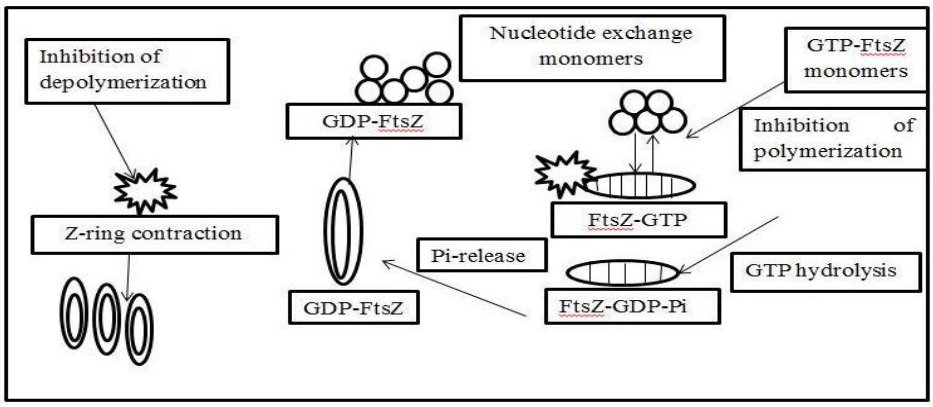

GTP- Guanosine-5'-Triphosphate; GDP- GuanosineDiphosphate

Fig. (1): The workflow of Filamentous Temperature Sensitive Mutant Z Gene (FtsZ).

MATERIALS AND METHODS

Using the software SYBYL X1.3, the molecule sketching and modelling calculations were carried out. Energy minimization was performed using Powell method with N.B. cut off 8.0 and dielectric constant 1.0 and was applied to all the compounds that were taken from the literature.

DATA SET

From the literature, a set of 48 molecules using the series of 2,5,6-tri-substitued benzimidazole derivatives related to anti-TB activity was taken. The data was converted into pIC_{50} and was used as dependent variable, for PLS analysis. The data set was manually selected following 80:20 ratio formula that is 34 molecules for training set and 14 molecules for test set was selected for the development of QSAR models.[8,9] Table 1 represents the molecules for the test and training sets.

Table (1): 2D structures for Filamentous temperature sensitive mutant Z gene (FtsZ) targeting Mycobacterium Tuberculosis.

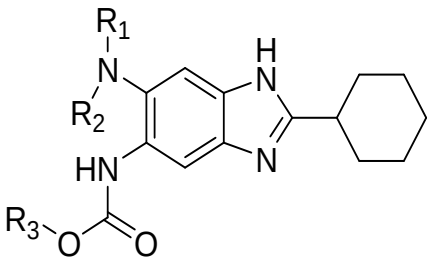

Sr.no	R_1R_2	R_3	pIC_{50}
1	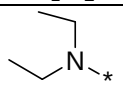	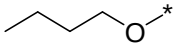	6.25
2	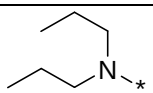	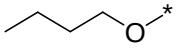	100
3*	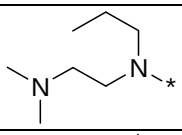	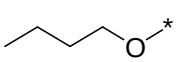	50.0
4	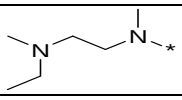	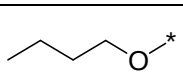	0.06
5		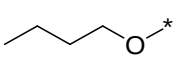	0.16
6		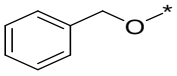	3.13

7*		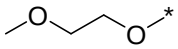	1.56
8*	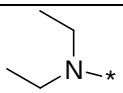	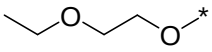	1.56
9*	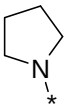	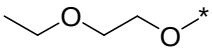	0.31
10		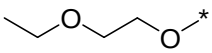	12.5
11*	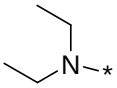	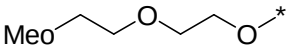	1.56
12*	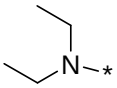	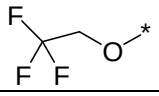	0.31
13		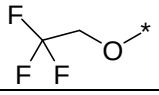	0.63
14		5l. 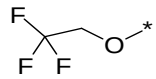	0.63
15	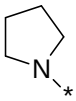	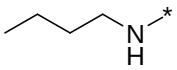	25.0
16	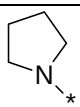	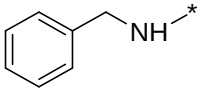	25.0
17*	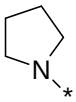	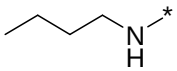	100
18	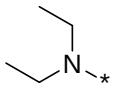	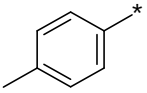	12.5
19	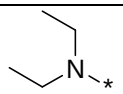	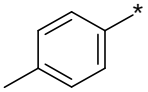	1.56
20*	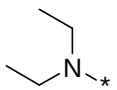	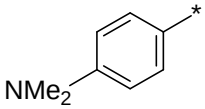	12.5
21*	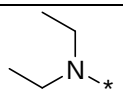	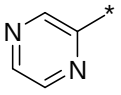	10.0
22	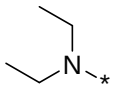	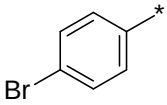	100
23	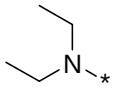	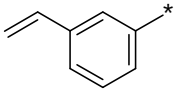	25.0

24*	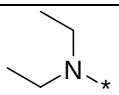	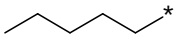	12.5
25	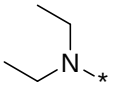	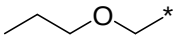	25.0
26	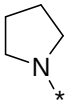	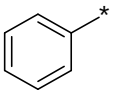	6.25
27*	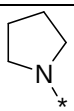	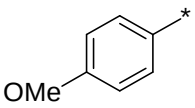	6.25
28	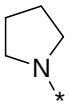	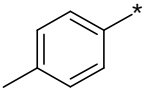	3.13
29	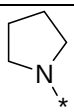	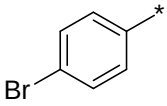	1.56
30	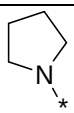	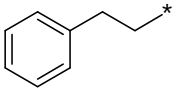	12.5
31*	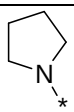	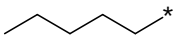	6.25
32*	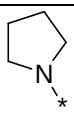	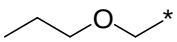	12.5
33*		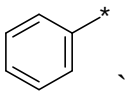	1.56
34*		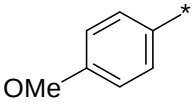	0.31
35		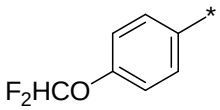	0.31
36		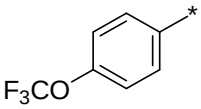	0.`16
37		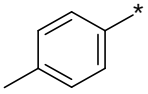	0.31
38		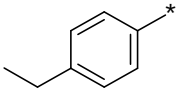	0.16
39		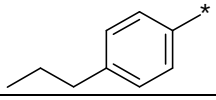	0.63

40		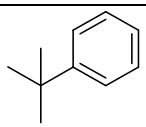	1.56
41		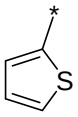	5.0
42		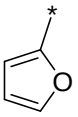	6.25
43		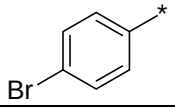	0.31
44		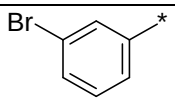	3.13
45		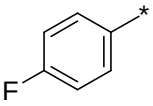	0.63
46		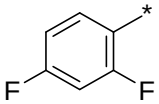	0.31
47		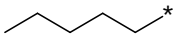	1.25
48		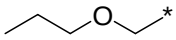	6.25

BIOLOGICAL ACTIVITY

As per the literature it can be known that the biological activity was carried out on the series of 2,5,6-tri-substituted benzimidazole derivatives using the Alamar Blue Assay technique. The cell line used was H37Rv as reported in the literature survey.[5] This method developed acts as a non-toxic, by using thermally stable reagent with good co-relation co-efficient.[3,5]

MOLECULAR ALIGNMENT TECHNIQUE

In order to obtain the finest confirmers for each molecule or compound, SYBYL X1.3 software was used for the modelling of compounds and optimization parameters. Using the Tripos Force Field with 1000 interactions all structures of the compounds were preliminary subjected into geometric optimization. Gasteiger-Huckel technique was used to calculate the partial atomic charges, with energy gradient plot of 0.05 kcal/molA^{o}. Hence, using this strategy the lowest energy conformer number 17 was chosen as template structure for the alignment of the data sets. It is rightly known, that molecular alignment technique is considered to be one of the most important step for the development of CoMFA and CoMSIA models. Hence, the technique was performed using distil arrangement method. Thus, rigid-

body fit was used, where the remaining compounds were super-imposed on each other in SYBYL X1.3.[8,9] (Fig. 2).

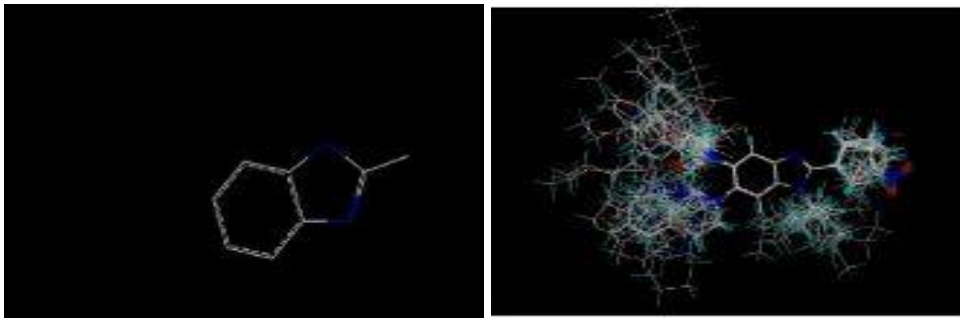

(A) **(B)**

Fig. (2): Molecular alignment. (A) Common structure retrieved from compound 17; (B) Alignment of the compounds in the training set.

CoMFA METHOD

The CoMFA method is commonly used to define the steric and electrostatic fields. Using the SYBYL X1.3 the procedure was carried out. Both fields were calculated at each lattice point with a grid spacing of 2.0 A^o using sp^3 hybridized carbon molecule with +1 charge acting as a probe with Van Der Waals radius of 1.52A^o and a charge of +1.00. Finally, column filtering was done by setting the filters to 1.0 and 2.0 kcal/mol latter, used as a optimal parameters of this model.[10]

CoMSIA METHOD

The CoMSIA method is similar to CoMFA in respect to the descriptors around aligned molecules. Three other fields (Hydrophobic, Hydrogen Bond Acceptor and Donor) were calculated as the same setting utilized in CoMFA calculations. Most imperatively, the Gaussian function is used to measure the distance between test molecule and each molecule atom.[10]

PLS ANALYSIS

The Partial Least Square Analysis (PLS) was carried out to determine the ideal number of components. The cross validated co-efficient q^2, acts as an internal statistical index of predictive power, was obtained. Thus, to predict the real predictive ability of the respective model derivatives by training set, biological activities of the test sets were predicted. The boot strapping by keeping 100 runs with column filtering of 2.0 kcal/mol was performed by generating new data sets from current data sets.[10] The quality of external prediction was

reported utilizing standard error of estimation (R^2), Q^2 and R^2 was calculated using the equation:

$$r^2_{pred} = SD\text{-}Press/SD$$

Where,

SD = sum of square deviation between the biological activity of molecules in test set and mean of biological activity of training set. PRESS= sum of square deviations between predicted and actual activity values for every molecule in the test set.

RESULT AND DISCUSSION

CoMFA and CoMSIA Outcome

The 3D-QSAR models were developed using the training set of 34 compounds and test set of 17 compounds. The statistical parameters related with CoMFA and CoMSIA is revealed in table 1. Subsequently, different alignment strategies can lead to distinctive statistical values in the developed QSAR models. The leading CoMFA and CoMSIA models were produced using a Partial Least Square (PLS) analysis, which produced cross-validated co-efficient (q^2). When a cross-validation co-efficients, $q^2 > 0.5$ was utilized, the model demonstrated statistical significance In Table 2, two descriptor fields in CoMFA form the combination models, that is steric and electrostatic fields. The CoMSIA models with combination of five descriptor fields, including steric, electrostatic, hydrophobic, hydrogen bond donor and acceptor were developed to create the optimal 3D QSAR models, still over-fitting appeared to happen for few models (those with a large number of components). From Table 2, it can be noted that the established models (CoMFA and CoMSIA) show high q^2 (0.627, 0.678), r^2 (0.968, 0.971), and F-values (522.74,302.32) along with a low standard error of estimate (SEE) (0.037, 0.117) and suitable number of components (6) which demonstrated good co-relation co-efficient (r^2_{pred}) including their corresponding test set molecules. The produced CoMFA and CoMSIA models with maximum external predictive ability (r^2_{pred} : 0.539, 0.565), were considered the best models. As shown in the fig. 3, the actual predicted pIC_{50} values of test and training sets for CoMFA and CoMSIA are noted. The CoMFA and CoMSIA models possess a good Q_{fit} with the clear diagonal line. Both the models too displayed satisfactory results throughout test and training sets.

Table (2): Statistical parameters of the CoMFA and CoMSIA models.

Parameter	CoMFA	CoMSIA
q^2	0.627	0.678
r^2_{ncv}	0.968	0.971
r^2_{cv}	0.647	0.619
r^2_{bs}	0.997	0.990
No. of components	6	6
F-values	522.74	305.32
SEE	0.037	0.117
r^2_{pred}	0.539	0.565
Field Contribution	-	-
Steric	0.468	0.170
Electrostatic	0.532	0.171
Hydrophobic	-	0.221
Hydrophobic Donor	-	0.261
Hydrophobic Acceptor	-	0.178

Leave-one-out cross-validated correlation co-efficient (q^2), noncross-validated correlation co-efficient (r^2), standard error of estimate (SEE), Fischer test values (F), steric field (S), electrostatic field (E), hydrophobic field (H), hydrogen bond donor (D), hydrogen bond acceptor (A).

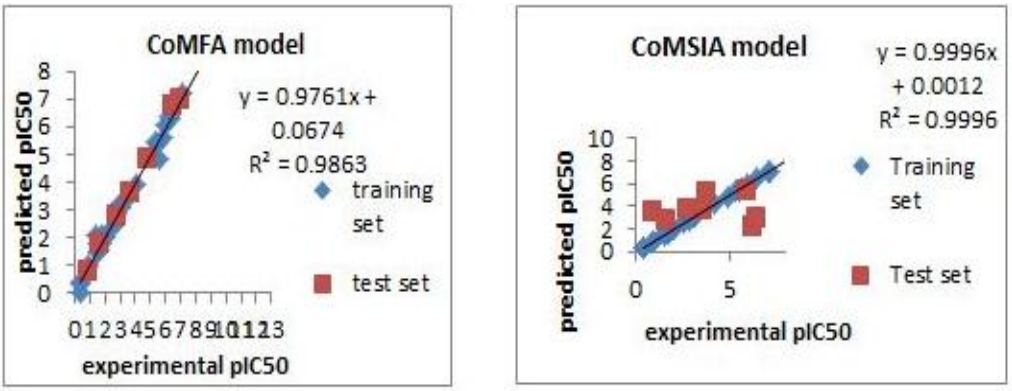

(A) **(B)**

Fig. (3): Plots of Actual versus predicted pIC_{50} values, for the training set and test set compounds, for CoMFA (A) and CoMSIA (B) models.

Interpretation of CoMFA

From the contour maps seen in figure, the analysis of CoMFA contour maps divulge that there is a significant green polyhedron at the para position of the structure. At this region it indicates bulky group and favours at R_1, R_2, and R_3 position. It is shown that benzene ring attached to five membered ring may increase its activity. Close to it is a big yellow polyhedron which signifies less bulkier group and enhance its activity. Red polyhedron at R_3

position indicates, will increase its negative charge at this position and expected to improve its activity. Moreover, electro negative halogen substituents (F, Br, etc) possess better active molecules instead of H at some compound in this position. Subsequently, at this region it increases its affinity by electron withdrawing groups like OCF_3 and $OCHF_2$ support this fact. Hence, more clear regions are seen with separate analysis of steric and electrostatic contour maps in Fig.4, respectively.

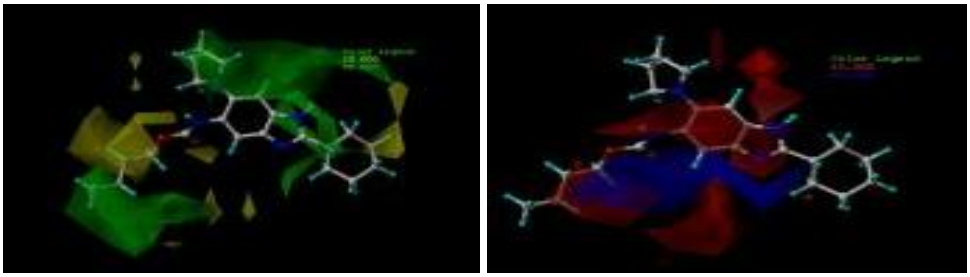

(A) **(B)**

Fig. (4): CoMFA contour maps displayed with potent compound, 17. (A) CoMFA steric contour map (green, favoured; yellow, disfavoured); (B) CoMFA electrostatic contour map (blue, electropositive favoured; red, electronegative favored).

Interpretation of CoMSIA

From the contour maps, the analysis of steric and electrostatic contour maps of CoMSIA models were similar to CoMFA contour maps. However, green colour possess steric field, blue colour favoured region while yellow and red colour is disfavoured near the functional group. In the yellow region, benzene ring depicts the requirement of less substituents and near R_3 position green colour favours bulky substituents. In case of electrostatic field, blue colour near benzene ring possess electron donating group is constrained at this position. As for the electrostatic field, the blue and red polyhedrons were found to be similar likewise of CoMFA models. While, at hydrophobic interaction, white colour indicates that benzene ring is active and bestows in the liphophilicity region. Whereas, yellow colour near unsaturated cyclic ring is disfavouring. The cyan and purple region indicates favours and disfavours in hydrogen bond donor interaction. But at R_3 position, cyan colour favours increases in activity and potency of respective compounds. In hydrogen bond acceptor, red colour depicts disfavoured region at acceptor group attached to carbonyl part while magenta colour near unsaturated cyclic ring favours biological activity. Hence, more clear regions are seen with separate analysis of steric, electrostatic, hydrophobic, hydrogen bond donor and acceptor contour maps in Figure 5, respectively.

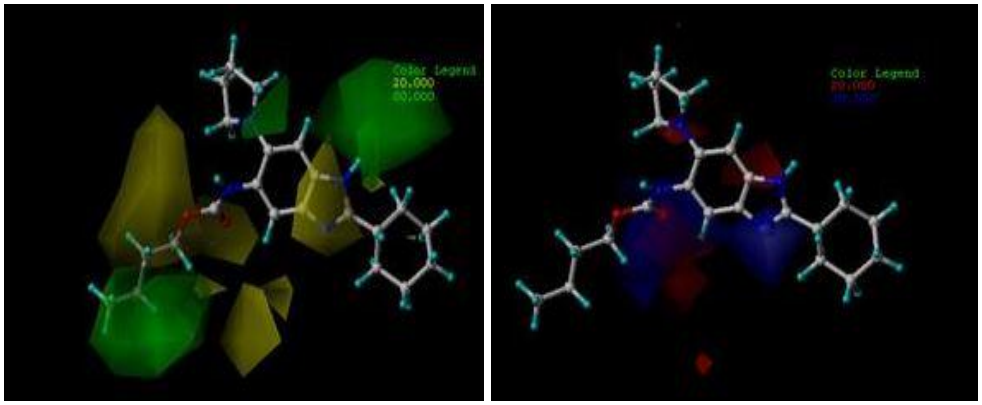

(A) (B)

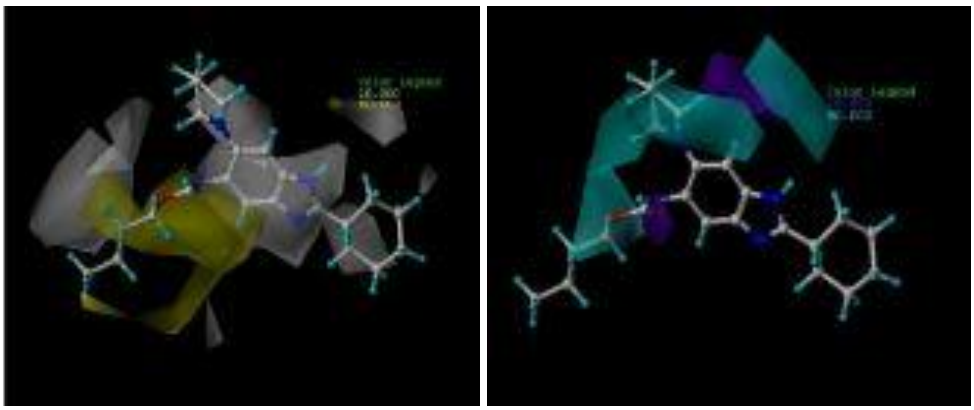

(C) (D)

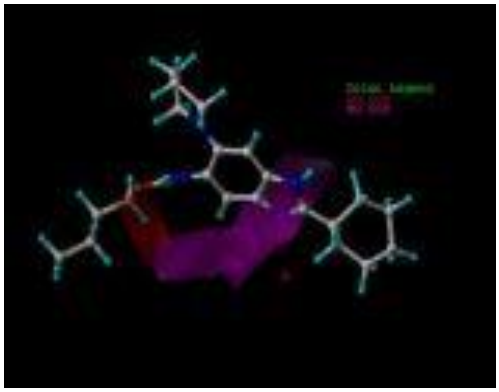

(E)

Fig. (5): CoMSIA contour maps displayed with potent compound, 17. (A) CoMSIA steric contour map (green, flavoured; yellow, disfavoured); (B) CoMSIA electrostatic contour map (blue, electropositive favoured; red, electronegative favoured); (C) CoMSIA hydrophobic contour map (yellow, favoured; white disfavoured); (D) CoMSIA hydrogen donor contour map (cyan, favoured; purple, disfavoured); (E) CoMSIA hydrogen acceptor contour map (magenta, favoured; red, disfavoured).

REFRENCES

1. Kalalbandi VKA, Seetharamappa J, Katrahalli U, Bhat KG. Synthesis, crystal studies, anti-tuberculosis and cytotoxic studies of 1-[(2E)-3-phenylprop-2-enoyl]-1H-benzimidazole derivatives.
2. Joshi SD, More UA, Pansuriya K, Aminabhavi TM, Gadad AK. Synthesis and molecular modeling studies of novel pyrroleanalogs as antimycobacterial agents.
3. Camacho J, Barazarte A, Gamboa N, Rodrigues J, Rojas R, Vaisberg A, et al. Synthesis and biological evaluation of benzimidazole-5-carbohydrazide derivatives as antimalarial, cytotoxic and antitubercular agents.
4. Jadhav GR, Shaikh MU, Kale RP, Shiradkar MR, Gill CH. SAR study of clubbed [1,2,4]-triazolyl with fluorobenzimidazoles as antimicrobial and antituberculosis agents.
5. Awasthi D, Kumar K, Knudson SE, Slayden RA, Ojima I. SAR Studies on Trisubstituted Benzimidazoles as Inhibitors of *Mtb* FtsZ for the Development of Novel Antitubercular Agents.
6. Masand VH, Jawarkar RD, Mahajan DT, Hadda TB, Sheikh J, Patil KN. QSAR and CoMFA studies of biphenyl analogs of the anti-tuberculosis drug (6S)-2-nitro-6-{[4-(trifluoromethoxy)benzyl]oxy}-6,7-dihydro-5H-imidazo [2,1-b][1,3]oxazine (PA-824).
7. Jian Y, He Y, Yang J, Han W, Zhai X, Zhao Y, et al. Molecular Modeling Study for the Design of Novel Peroxisome Proliferator-Activated Receptor Gamma Agonists Using 3D-QSAR and Molecular Docking.
8. Kumar K, Awasthi D, Berger WT, Tonge PJ, Slayden RA, Ojima I. Discovery of anti-TB agents that target the cell-division protein FtsZ.
9. Kouassi A, Kone M, Keita M, Esmel A, Megnassan E, N' Guessan Y, et al. Computer-Aided Design of Orally Bioavailable Pyrrolidine Carboxamide Inhibitors of Enoyl-Acyl Carrier Protein Reductase of Mycobacterium tuberculosis with Favorable Pharmacokinetic Profiles.
10. Zhao X, Chen M, Huang B, Ji H, Yuan M. Comparative Molecular Field Analysis (CoMFA) and Comparative Molecular Similarity Indices Analysis (CoMSIA) Studies on α1A-Adrenergic Receptor Antagonists Based on Pharmacophore Molecular Alignment.